ADVANCED FUNCTIONAL MATERIALS
www.afm-journal.de

Electrochemical Quantification of *Escherichia coli* with DNA Nanostructure

Marcella Giovanni, Magdiel Inggrid Setyawati, Chor Yong Tay, Hang Qian, Win Sen Kuan, and David Tai Leong**

***Escherichia coli* is an indicator of fecal contamination in recreational water and some strains are responsible for serious food poisoning in humans. Therefore, having a rapid, sensitive, selective, and simple *E. coli* detection is important. In this study, DNA nanopyramids anchor is utilized for immunological detection of *E. coli* lipopolysaccharides, lysate, and whole bacteria. By measuring the *E. coli* amount electrochemically, detection limits of 0.20 ng mL^{-1} *E. coli* lipopolysaccharides and 1.20 CFU mL^{-1} equivalent of lysed *E. coli* bacteria are obtained. Our method confers selectivity to detect *E. coli* in the presence of various other macromolecules. Therefore, our system can be developed to test the *E. coli* content in real water samples.**

1. Introduction

Escherichia coli is commonly found in the human gut and usually excreted together with fecal matter. The presence of *E. coli* in various water supply sources is used as an indicator of coliform and fecal matter contamination in drinking water and recreational water in freshwater lakes as recommended by the World Health Organization (WHO). While most *E. coli* strains are harmless to their hosts,[1] pathogenic *E. coli* strains still pose major public health concerns. From 2011 to 2013 alone, outbreaks resulting from ingested pathogenic *E. coli* had given rise to over 4000 cases with more than 50 fatalities worldwide.[2] The presence of *E. coli* in food is not only from animal-sourced food stock but also from vegetables grown in *E. coli*-infested soil and water. Thus, it is important to obtain a rapid, sensitive, and specific technique for *E. coli* determination.

M. Giovanni, M. I. Setyawati, Dr. C. Y. Tay, Dr. H. Qian, Prof. D. T. Leong
Department of Chemical and Biomolecular Engineering
National University of Singapore
4 Engineering Drive 4, Singapore 117585, Singapore
E-mail: cheltwd@nus.edu.sg
Dr. W. S. Kuan
Department of Surgery
Yong Loo Lin School of Medicine
National University of Singapore
Emergency Medicine Department
National University Hospital
National University Health System
5 Lower Kent Ridge Road, Singapore 119074, Singapore
E-mail: win_sen_kuan@nuhs.edu.sg

DOI: 10.1002/adfm.201500940

Many techniques have been developed to determine the number of *E. coli* in various water samples. Methods from the traditional agar culture and plate count to the more modern chemical reactivity-based techniques in detecting nucleic acid, polymerase chain reaction (PCR), immunological probing such as enzyme-linked immunosorbent assay (ELISA), as well as nanoparticle-based biosensing and potentially therapeutic methods[3] have been evaluated for their speed, accuracy, and selectivity in order to help regulate the allowable level of *E. coli* content in water. The United States Environmental Protection Agency has recommended that the acceptable *E. coli* content to be less than 1.26 colony forming unit (CFU) in 1 mL of recreational water,[4] while WHO proposed that drinking water must be free of *E. coli* and other coliforms.[5] At such low concentrations, there are not many technical options for rapid determination of *E. coli* concentration in water left, except PCR-based techniques. The PCR reaction could overcome the low concentration issues through amplification of the bacterial specific genes. However, the need for purified samples automatically necessitates extensive purification steps prior to the PCR reaction. It is precisely because PCR also has a very powerful amplification step that it also suffers from amplification of false-positive signals. In addition, *E. coli* DNA as a marker through PCR amplification is so stable that even DNA from nonviable *E. coli* may give an overly conservative measure of the amount of *E. coli* in the samples. A possible solution to these problems is an ultrasensitive system that does not require any signal amplification or purification steps and yet robust and sensitive enough for routine testing of water-borne bacteria.

Electrochemical readouts have widely been employed in the detection of pathogens in food and water samples, as well as for medical diagnosis.[6] Voltammetric analysis that makes use of reduction–oxidation (redox) reaction is one of the popular bacteria electrochemical detection methods. One idea is to use β-galactosidase produced by *E. coli* as a means to mediate the oxidation of *p*-aminophenyl galactopyranoside (pAPG) to *p*-aminophenol (pAP). The oxidation process generates electrons for subsequent amperometric detection, resulting in a limit of detection (LOD) of 10 CFU mL^{-1}.[7] However, β-galactosidase-based detection of *E. coli* requires expansion of the bacteria for several hours and pretreatment steps to obtain meaningful signal for low initial bacteria concentration.[8] As such, in this study we choose to utilize lipopolysaccharide (LPS), a major

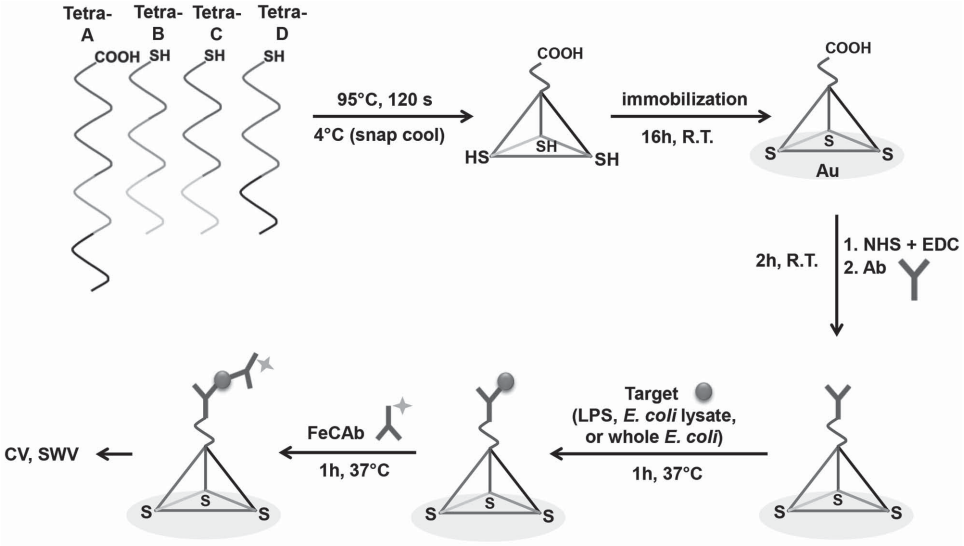

Figure 1. Schematic of the assembly method.

component of *E. coli* membrane, as a target. The use of LPS as an antigen in the detection strategy of immuno-based voltammetry allowed the development of a specific detection system with rapid and sensitive readout.

DNA nanostructures have garnered much interest for analytical method development. Their self-assembled structures are predictable as they are designed based on well-understood A-T and C-G base pairing. Moreover, the core structure of DNA comprising bases, sugar molecules, and phosphate groups makes them relatively easy to conjugate with various tags and functionality,[3c–3f] thus enhancing their flexibility for many applications outside DNA's perceived traditional role as genetic information storage.[3c–3f] For electrochemical applications, the DNA nanostructure can be immobilized onto a gold (Au) surface via a thiol group attached at either the 3′ or 5′ terminus, which subsequently allows the formation of self-assembled monolayer of DNA nanostructure at the Au surface via a single-point anchor.[9] Through a proper design, it is possible to orientate the DNA nanostructure to achieve its intended use. To improve probe-target recognition, Pei et al.[10] proposed the use of a tetrahedral shape. The probe is expected to bind to the Au surface via the aforementioned thiol–Au bond at three different vertices, leaving one vertex available for conjugation with other moieties. In particular, we have earlier demonstrated that a DNA nanopyramid (DP)-based IgG detection system could selectively distinguish IgG in a protein cocktail with a limit of detection of 2.8 pg mL^{-1}.[11] This superior ability was attributed to the theoretical regular spatial separation of 4 nm when DPs are anchored on the electrode surface. The hollow structure of the DP enhanced the electron transfer capability from the redox tag, ferrocene (FeC), to the electrode surface, when compared to other commonly used anchors such as a long hydrocarbon chain mercaptoundecanoic acid.

In this article, we described an ultrasensitive, antibody-based electrochemical biosensor to determine the concentration of *E. coli*. The DP served as an anchor for goat anti-*E. coli* antibody (Ab). **Figure 1** depicts the schematic of the detection assembly process. First, the Ab was immobilized onto the remaining vertex of the DP anchor and due to the stable and designed height from the surface, the Ab then projects easily to capture the antigens specifically, namely *E. coli* LPS, *E. coli* bacteria lysate, or whole *E. coli* bacteria. FeC-conjugated Ab (this moiety will be referred to as "FeCAb" in subsequent mentions) was finally added to complete the sandwich immunosensor assembly by recognizing the target assembled to the DP-antibody structure on the electrode surface, hence allowing a specific detection of the target. By using this method, we are able to distinguish even one whole *E. coli* bacterium. In addition, we achieved LODs of 0.20 ng mL^{-1} LPS and bacteria lysate obtained from 1.20 CFU mL^{-1} *E. coli*. The LODs are close to the standards set by WHO.

2. Results and Discussion

2.1. Characterization of Detection Components

2.1.1. Preparation of DP and FeCAb

DP were assembled and validated with polyacrylamide gel electrophoresis (Figure S1, Supporting Information). We also conjugated FeC to Ab as an electroactive tag for the electrochemical detection and quantification of the various targets. The successful formation of FeCAb was analyzed by using UV–vis spectrophotometry. As plotted in **Figure 2**A, FeC alone exhibited characteristic peaks at 254, 299, and 433 nm, while Ab showed a peak at 280 nm that is the typical absorption wavelength of proteins. After conjugation, we observed the presence of peaks at 260 nm with the disappearance of the FeC peak at 299 nm and Ab peak at 280 nm. The appearance of this additional peak at the purified synthesis product may be due to the combination of peaks from Ab and FeC that signified the successful conjugation of FeC to Ab.

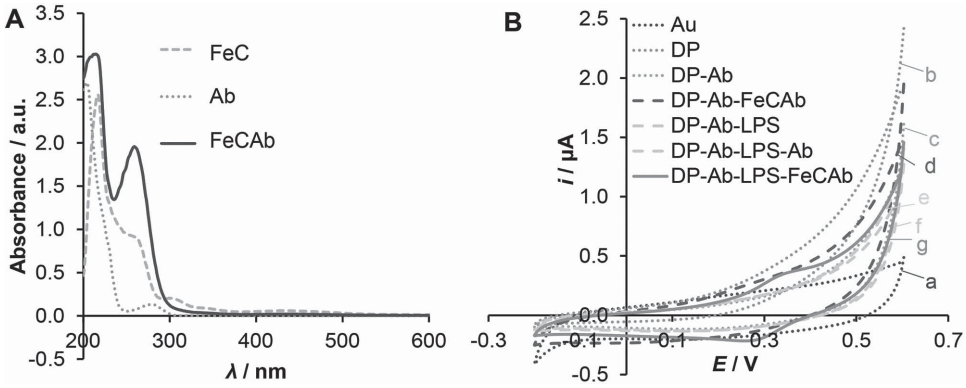

Figure 2. Characteristics of various components involved in the DP-based *E. coli* detection assembly. A) UV–vis spectra of FeC, Ab, and FeCAb. B) Cyclic voltammetry characterizations of a) bare Au electrode and the electrode modified with the detection assembly namely b) DP, c) DP and Ab, d) DP, Ab, and FeCAb (without any target), e) DP, Ab, and LPS, f) DP, Ab, LPS, and Ab (without FeC), and g) DP, Ab, LPS, and FeCAb (complete detection assembly). Electrochemical signal coming from the electroactive tag FeC comes about only when both the target and FeCAb are present and recognize each other in the specific antibody–antigen interactions (curve g), as shown by the absence of signals when FeCAb is added to the detection system without target (curve d) and when Ab (without FeC) is added to the detection system with target (curve f). Concentration of LPS used is 5 ng mL^{-1}. All potentials are stated versus Ag/AgCl reference electrode.

2.1.2. Antibody–Antigen Specificity

We probed the Ab (primary antibody) and whole *E. coli* complex with a fluorescent secondary antibody recognizing the Ab. Positive secondary–primary antibodies recognition would signify the successful primary antibody and target recognition, hence proving the specificity of our antibody to our target. As shown in Figure S2A (Supporting Information), red fluorescence is observed in place where the bacteria were deposited (blue fluorescence). The red fluorescence came from the Alexa Fluor dye that is conjugated to the anti-goat antibody, probing for the goat anti-*E. coli* antibody used in this study. This shows that our Ab could recognize its target well. To ascertain that the fluorescence observed was not due to nonspecific binding between the secondary antibodies and the target, we performed a control experiment in which the secondary antibody was directly added to the whole *E. coli* (no addition of primary antibody) and showed that no fluorescence was observed (Figure S2B, Supporting Information). Hence, it is ascertained that the choice of antibody and antigen was appropriate for the detection.

Interestingly, only the outer membrane of *E. coli* fluoresced (inset to Figure S2A in the Supporting Information). We postulated that the antigen for the detection is on the surface of *E. coli*. Therefore, it is possible to detect the components of bacterial membrane, such as LPS rather than whole bacteria, and obtain the equivalent result of the presence of the whole bacteria using its membrane components. For subsequent experiments on the optimization of the detection assembly, we decided to use LPS as the model target for the *E. coli* quantification as the target is smaller than the other two targets, bacteria lysate and whole bacteria, thereby reducing the complexity of the detection arising from the shape and size of the bacteria.

2.1.3. Signal Generation from the Detection Assembly

Figure 2B shows the generation of electrochemical signals due to the complete assembly of the sandwich immunosensor, comprising DP, Ab, LPS target, and FeCAb when recorded with cyclic voltammetry (CV). A pair of oxidation and reduction peaks at +0.3 V and +0.4 V, respectively, appeared that corresponds to the FeC redox potentials upon the formation of a complete immunosensor with LPS (curve g) as the target. We noted that the peaks did not appear when an unconjugated Ab was added in place of FeCAb (curve f), which confirmed that the source of these peaks is from the FeC moiety that successfully completed the sandwich structure. Also, when the FeC-conjugated Ab was added to the DP-Ab construct without the target (curve d), there was no observable peak; hence, we could be certain that no nonspecific binding had interfered with the detection. We also did not observe any discernible oxidation and reduction peaks from the Au electrode alone (curve a) and when the assembly consists only of DP (curve b), DP-Ab (curve c), and DP-Ab-LPS (curve e). Therefore, it can be determined that the detection of antigens was made possible only in the presence of both the FeCAb and the target. Additionally, other detection components do not interfere with the signal. Similar observations were made when we attempted to characterize the signal generation with addition of *E. coli* lysate and whole *E. coli* bacteria in place of the LPS (Figure S3, Supporting Information).

2.2. Detection of LPS

As measuring the presence of LPS with Ab gave us a redox peak due to the complete detection assembly (Figure 2B), we attempted to perform LPS detection by using square wave voltammetry (SWV) to measure the current generated when the electroactive tag, in this case FeC, undergoes oxidation (typical voltammogram is shown in **Figure 3**A). This current correlates to the amount of target present. We chose SWV as the detection method because this technique is known to be able to generate higher current signals compared to other voltammetric techniques such as CV and differential pulse voltammetry,[12] indicating that the technique can aid more sensitive measurement

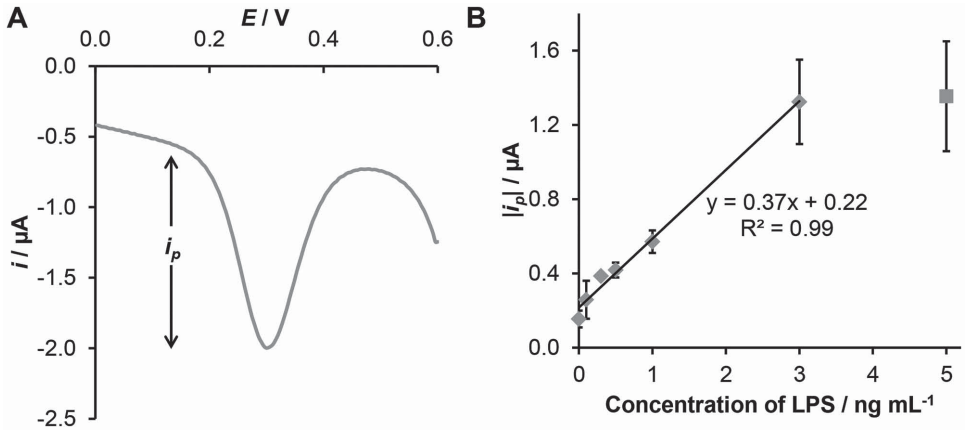

Figure 3. SWV detection of LPS. A) The typical square wave voltammogram for the detection of LPS (3 ng mL^{-1}). The peak at +0.3 V (vs Ag/AgCl) corresponds to the oxidation peak of FeC, the electroactive tag used to realize the detection. i_p refers to the magnitude of the peak current. Potentials are stated versus Ag/AgCl reference electrode. B) The peak current responses (in absolute values) for the detection of LPS as measured with SWV, with a linear range from 0 to 3 ng mL^{-1} of LPS. Error bars refer to standard deviations from three independent experiments.

of electroactive materials, resulting in an electrochemical system's ability to reach lower LOD. From Figure 3B, we showed that the increasing concentration of LPS from 0 to 3 ng mL^{-1} gave a linear peak current response (R^2 = 0.99). The signal reached plateau beyond 3 ng mL^{-1}. Our method achieved an LOD of 0.20 ng mL^{-1}.

2.3. Detection of *E. coli* Lysate

Our system's ability to quantify LPS, a small target found on the outer bacterial membrane, prompted us to study the system's ability to quantify LPS found in the complex mixture of *E. coli* lysate. A sensitive quantification of *E. coli* lysate would result in more efficient *E. coli* detection using our system, as lysing bacteria is much easier and faster than obtaining purified LPS from samples. As shown in **Figure 4**A, we were able to detect *E. coli* lysate from as low as 1 CFU mL^{-1} whole bacterium lysate equivalence. A logarithmic value of lysate concentration was observed to be linearly correlated with the current response (R^2 = 0.98, Figure 4B) from 1 to 100 CFU mL^{-1} equivalent of *E. coli* bacteria lysed. We achieved an LOD of *E. coli* lysate concentration equivalent to 1.20 CFU mL^{-1} of *E. coli*, which is lower than the LOD obtained by other electrochemical-based *E. coli* quantification methods.[13] Our LOD is also below the WHO-determined *E. coli* content standard in recreational water of 1.26 CFU mL^{-1}, which will be excellent for analysis of real water samples without the need of preconcentration or dilution.

2.4. Detection of Whole *E. coli* Bacteria

We attempted to detect whole *E. coli* with our detection system, and the result is plotted in **Figure 5**A. Similar to the quantification of *E. coli* lysate (Figure 4), we were able to distinguish the presence of even a single bacterium as the peak current increased by 3.5-fold than the control (i.e., no target added). We also obtained an excellent linearity between the logarithmic value of bacteria concentration with the current response (R^2 = 1.00; Figure 5B) from 1 to 100 CFU mL^{-1}, which is the same linear range as for the detection of *E. coli* lysate. Therefore, our system gives good agreement in detecting various forms of *E. coli*. However, the much less steep standard curve slope of whole bacteria detection as compared to those of LPS

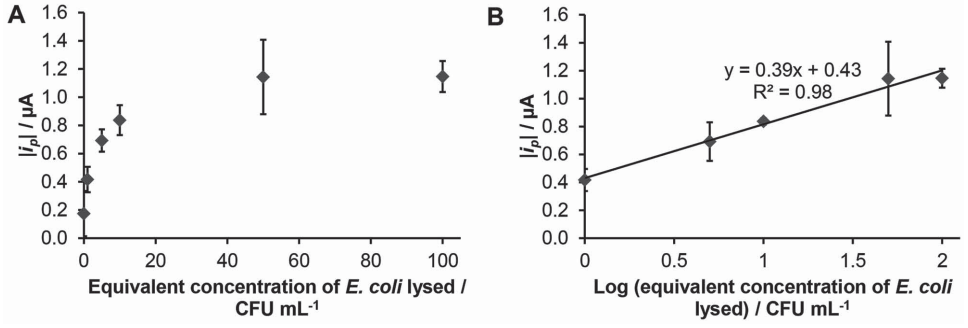

Figure 4. SWV detection of *E. coli* lysate. A) The absolute values of peak current responses for the detection of *E. coli* lysate were measured with SWV. B) The linearity between the logarithmic value of target concentration with the current generated. Error bars refer to standard deviations from three independent experiments.

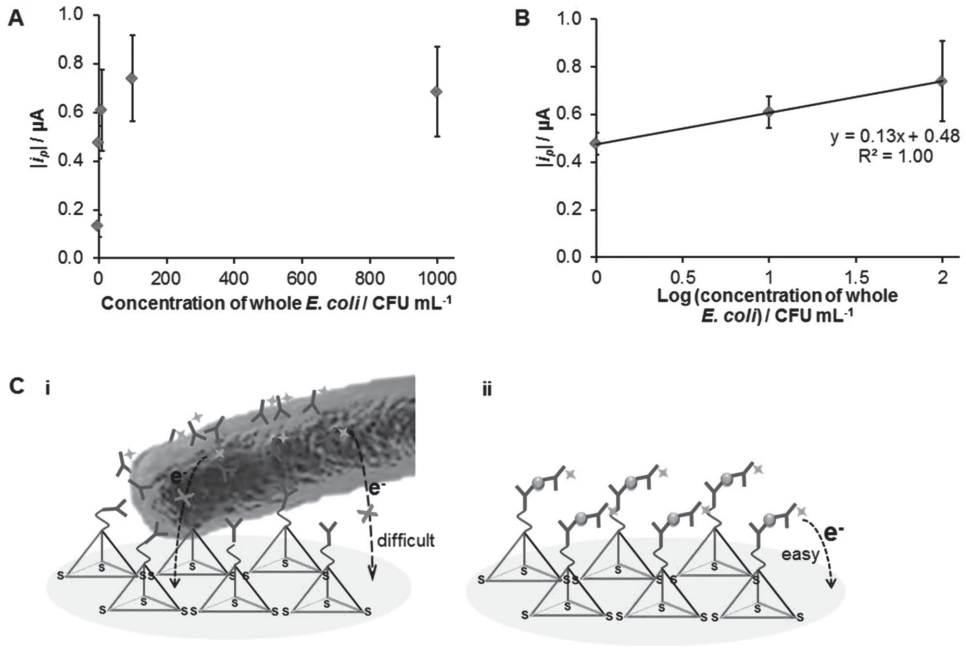

Figure 5. SWV detection of whole *E. coli* bacteria. A) The absolute peak current responses for the detection of whole *E. coli* bacteria as measured with SWV. B) The linearity between the logarithmic value of target concentration with the current generated. Error bars refer to standard deviations from three independent experiments. C) Schematics depicting i) the difficulty of electron transfer from FeC electroactive tag to the Au electrode surface when whole *E. coli* was detected, and ii) the ease of the same electron transfer when small targets (LPS and *E. coli* lysate) were detected. The size and shape of the whole bacteria may cause it to cover multiple Ab and block the access of electrons to the electrode, while the more compact size and shape of the smaller targets still allow some space for the electron transfer.

and lysate detections (0.13 for whole *E. coli* detection vs 0.37 of LPS detection and 0.39 of lysate detection) implied that the system exhibits less sensitivity for discerning the signal resulting from one concentration of *E. coli* with another in comparison for the detection of the other two targets. We attributed this to the comparatively more compact size and shape of LPS molecules in bacteria lysate (that essentially is whole bacteria that have been sheared) than in whole bacteria, and the latter can saturate the electrode surface.[14] As depicted in Figure 5C(i), the whole bacteria binding hampers the electron transfer from the FeC tag to the electrode, a feature that is not present when the smaller targets are detected (Figure 5C(ii)). We also postulated that the bacteria could bind to more than one Ab since it has relatively much bigger size than the probes (1 µm of whole *E. coli* in length vs 6 nm scalewise of the Ab and DP construct) and pose as a nonconductive barrier to electron transfer. The bacteria can also bind to more than one FeCAb that may explain the high jump in peak current in the detection of a single bacterium, even though not all electrons resulting from the oxidation of FeC can reach the electrode surface easily due to the huge distance between some of the redox probe to the electrode as well as the whole bacteria that saturate the electrode surface and act as a physical, nonconductive barrier to electron transfer. Therefore, while the system may be adequate to sense the presence of very low amount of bacteria, it might not be a robust quantification method. Lysing the bacteria would be a better option for quantifying the bacteria concentration in real samples.

2.5. Specificity of the Detection Assembly

Immunological detection involving specific antibody–antigen recognition is one of the most specific nonamplification detection methods known thus far. To prove the specificity of our system, we challenged our sensor when the target is suspended in a complex mixture of components represented by skim milk. As shown in **Figure 6**, our detection assembly could measure all the targets in skim milk at about the same current values as the target suspended in the buffer only. Electrochemical current comparable to the current from the control was observed when skim milk without bacteria was added. We ascertained that the presence of other components in skim milk does not interfere with the detection nor give false-positive results for the *E. coli* detection. The distinguishing ability is attributed to the specific interaction between Ab and *E. coli* components (LPS, lysate, or whole bacteria) that are not found in other mixture components. Our method could selectively measure *E. coli* in mixtures, avoiding the need for separating the *E. coli* from the mixture they are suspended in prior to quantification, thus speeding up the detection process.

Several reports on *E. coli* detection (**Table 1**) by using electrochemical impedance spectroscopy have achieved limit of detection (LOD) ranging from 2 to thousands CFU mL^{-1}.[13–15] Those using other types of electrochemical detection reported detection limits of more than 30 CFU mL^{-1}.[16] Our system, which can distinguish even one bacterium, is more sensitive than other nonamplified systems that were utilized for *E. coli* detection. A Raman spectroscopic method, though rapid, is

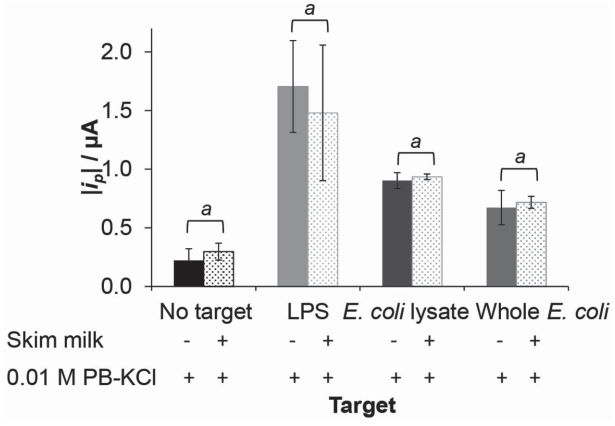

Figure 6. Targets (LPS, *E. coli* lysate, and whole *E. coli* bacteria) suspended in a complex mixture (represented by 1% skim milk in 0.01 M PB-KCl) do not give significant difference than their respective counterpart suspended in 0.01 M PB-KCl only. The absolute values of the peak current signals coming from 1% skim milk in 0.01 M PB-KCl without any target spiked in do not interfere with the signals coming from the target; thus, our sensing system can distinguish target in complex mixtures. Concentrations of LPS, lysate, and whole bacteria used are 5 ng mL^{-1}, 10 CFU mL^{-1} equivalent of whole bacteria lysed, and 100 CFU mL^{-1}, respectively. Data are plotted as the average of three independent measurements with the error bar corresponding to standard deviation. [a] $p > 0.05$ based on Student's *t*-test.

less sensitive with an LOD of 10 CFU mL^{-1} and less specific as well as requiring a sample processing step prior to the measurement.[17] PCR-based methods suffer from, among many others, membrane-clogging and contamination from mixture components.[18] Though separation of the bacteria from its solvent may be advantageous,[19] it requires additional steps that lengthen the overall process time and more steps increase the chance of random errors introduction. Employing our DP-based electrochemical immunosensing for *E. coli* detection is not only sensitive but also overcomes the issues of sensor specificity and interference from inherent sample complexity.

3. Conclusion

We have developed a DP-based electrochemical *E. coli* sensor through the use of anti-*E. coli* antibody. We have achieved LODs of 0.20 ng mL^{-1} of LPS from *E. coli* and 1.20 CFU mL^{-1} equivalent of *E. coli* that underwent lysis prior to detection. Our LODs are below the WHO-recommended *E. coli* content in water to ensure acceptable recreational water quality of 1.26 CFU mL^{-1}. In addition, our system could distinguish *E. coli* from other targets when they are suspended in a mixture. However, detection of whole *E. coli* bacteria was found to be good qualitatively but not quantitatively. Nonetheless, the excellent LOD of our system will enable it to be developed further to examine the recreational and drinking water quality with regard to fecal matter contaminant.

4. Experimental Section

Materials: All chemicals were used as received. Lipopolysaccharides from *E. coli* O111:B4 (LPS), *N*-hydroxysuccinimide (NHS), *N*-(3-dimethylaminopropyl)-*N′*-ethylcarbodiimide hydrochloride (EDC hydrochloride), Tris(2-carboxyethyl) phosphine hydrochloride (TCEP), 4-(2-hydroxyethyl) piperazine-1-ethanesulfonic acid (HEPES), and bovine serum albumin (BSA) were obtained from Sigma-Aldrich, USA. Tris base was obtained from 1st Base, Singapore. Magnesium chloride ($MgCl_2$), sodium dihydrogen phosphate (NaH_2PO_4), sodium hydrogen phosphate (Na_2HPO_4), potassium dihydrogen phosphate (KH_2PO_4), and potassium chloride (KCl) were purchased from Merck, Germany. Ferrocene (FeC) monocarboxylic acid was obtained from Santa Cruz Biotechnology, USA. Difco LB broth, Miller (Luria-Bertani) medium for *E. coli* growth, and Plate Count Agar were obtained from Becton, Dickinson, and Company, USA and Merck, Germany, respectively, and reconstituted to the respective solutions as per manufacturer's instruction. Anti-*E. coli* antibody from goat polyclonal to *E. coli* (Ab; catalog no. ab25823) and rabbit anti-goat antibody conjugated with Alexa Fluor 546 were purchased from Abcam, UK and Invitrogen, USA, respectively. Oligonucleotides strands were synthesized by Sigma-Aldrich, Singapore and AITBiotech, Singapore. Electrolyte solutions and wash buffers consisted of 0.1 M phosphate buffer supplemented with 0.1 M KCl (0.1 M PB-KCl; 0.1 M Na_2HPO_4, 0.1 M NaH_2PO_4, 0.1 M KCl, pH 7.4) and its ten times diluted preparation (0.01 M PB-KCl). All solutions were prepared in ultrapure water (Milli-Q; 18.2 MΩ cm at 25 °C, Merck Millipore, USA) unless otherwise stated.

Bacteria Culture: E. coli K12 bacteria strain stock (catalog no. 700926, American Type Culture Collection, USA) was grown in Luria-Bertani broth at 37 °C for 16 h with shaking at 200 rpm. The bacteria were then plated on Plate Count Agar to determine their concentration. For further detection experiments, the growth medium was removed and the bacteria were suspended in 0.01 M PB-KCl. For bacteria lysis, the bacteria were suspended in 0.01 M PB-KCl containing 1% protease inhibitor cocktail and then ultrasonicated for 6 × 10 s with 5 s intervals in an ice bath.

FeCAb Synthesis: The synthesis followed a published report.[11] Briefly, FeC monocarboxylic acid (2 mg), NHS (10 mg), and EDC (15 mg) were

Table 1. Current *E. coli* detection methods and their performance.

Method	Target	Limit of detection [CFU mL^{-1}]	Linear range [CFU mL^{-1}]	Ref.
DNA nanostructure-based/electrochemical	*E. coli* K12	1	$1–10^2$	This study
Polymer self-assembled monolayer-based/electrochemical	*E. coli* O157:H7	2	$3 \times 10^1–3 \times 10^4$	[13]
Carbohydrate-based/electrochemical	*E. coli* ORN178	10^2	$10^2–10^3$	[14]
Peptide-based/electrochemical	*E. coli* K12	10^3	$10^3–10^7$	[15]
Gold nanoparticles-based/electrochemical	*E. coli* O157:H7	3.4×10^2	$7.8 \times 10^1–7.8 \times 10^6$	[16a]
Polymer self-assembled monolayer-based/electrochemical	*E. coli* DH5α, *E. coli* HB101	6×10^2	$6 \times 10^1–6 \times 10^8$	[16b]
Surface-enhanced Raman spectroscopy	*E. coli* O157:H7	10^1	No information	[17]

Table 2. Sequences of oligonucleotides used to form the DP.

Name	Sequence (5′ to 3′)
Tetra-A	HOOC-TTTTTTTTTTACATTCCTAAGTCTGAAACATTACAGCTTGC-TACACGAGAA GAGCCGCCATAGTA
Tetra-B	HS-C6-TATCACCAGGCAGTTGACAGTGTAGCAAGCTGTAA TAGATGCGAGGGTCCAATAC
Tetra-C	HS-C6-TCAACTGCCTGGTGATAAAACGACACTACGTGGG AATCTACTATGGCGGCTCTTC
Tetra-D	HS-C6-TTCAGACTTAGGAATGTGCTTCCCACGTAGTGTCG TTTGTATTGGACCCTCGCAT

thoroughly dissolved in 50×10^{-3} M HEPES buffer, pH 7.3. After 2 h of stirring to activate the carboxyl group on the FeC, Ab (10 μg mL^{-1}) was added dropwise and the stirring continued for 12 h in room temperature. The mixture was then spun down at 5000 rpm for 10 min to remove the solids, and the supernatant was then purified by centrifugation at 10 000 ×*g* by using centrifugal concentrator device (MWCO 10K; Pierce Biotechnology, USA). The purified FeCAb was then stored at 4 °C until use.

DP Formation: The reaction procedure followed previous reports.[3c,11] DP was formed through annealing of four oligonucleotides strands, with three strands containing thiol group and one strand containing carboxyl group (sequences are listed in **Table 2**, detection schematic in Figure 1A). The four oligonucleotides strand as the DP constituents were mixed in TM buffer (20×10^{-3} M Tris, 50×10^{-3} M $MgCl_2$) and 7.5×10^{-3} M TCEP to reduce the disulfide bonds. The mixture was then heated to 95 °C for 2 min and then rapidly cooled down to 4 °C to assist the self-assembled formation of the tetrahedral structure.

DP-Based Sensor Assembly: The DP mixture (3 μL) was dropped onto a freshly cleaned Au working electrode surface (2 mm diameter; CH Instruments, USA) and left overnight to allow the anchoring of the DP on the Au surface through the strong thiol–Au bond. A mixture of 100×10^{-3} M NHS and 400×10^{-3} M EDC (total volume of 3 μL) was then deposited onto the electrode surface for 30 min to activate the carboxyl group on the DP to aid in the formation of amide bond between DP and the antibody as the sensing probe. Afterward, Ab (3 μL, 10 μg mL^{-1} in 0.01 M PB-KCl) was added to the electrode surface and let react for 2 h at room temperature. Blocking of excess surface was done with 1% BSA in 0.01 M PB-KCl for 30 min. 3 μL of target, either LPS, *E. coli* lysate, or whole *E. coli* bacteria suspended in 0.01 M PB-KCl (and also in 1% skim milk in 0.01 M PB-KCl for specificity study) was added and the recognition between Ab and target was carried out at 37 °C for 1 h. To complete the sandwich immunoassay, FeCAb (3 μL) was pipetted onto the electrode surface and the reaction was allowed to occur at 37 °C for 1 h. After the sandwich is complete, the electrodes were subjected to the respective voltammetric measurement.

Voltammetric Measurements: Cyclic voltammetry (CV) and square wave voltammetry (SWV) were performed on an Autolab PGSTAT302N (Metroohm B.V., The Netherlands) connected to a personal computer and controlled by General Purpose Electrochemical System software (Eco Chemie, The Netherlands). A standard three-electrode configuration of the Au working electrode, Ag/AgCl reference electrode, and platinum wire counter electrode (all electrodes were purchased from CH Instruments, USA) were used. All CV and SWV scans were recorded in 0.1 M PB-KCl. For CV, the scan range was from –0.2 to +0.6 V while for SWV, the signal was recorded from +0.6 to 0 V.

Supporting Information

Supporting Information is available from the Wiley Online Library or from the author.

Acknowledgements

The authors acknowledge Ministry of Education AcRF Tier 1 (R-297-000-414-112) and National University Health System Funding Support (NR13NEM220MP) through the Engineering-Medicine Seed Fund 2013 to D.T.L. and W.S.K. The authors thank Professor En-Tang Kang for allowing access to the electrochemical workstation. They declare no competing financial interests. The author titles were amended on July 1, 2015.

Received: March 9, 2015
Revised: April 8, 2015
Published online: April 30, 2015

[1] J. B. Kaper, J. P. Nataro, H. L. T. Mobley, *Nat. Rev. Microbiol.* **2004**, *2*, 123.
[2] N. Aboutaleb, E. J. Kuijper, J. T. van Dissel, *Curr. Opin. Gastroenterol.* **2014**, *30*, 106.
[3] a) G. A. Sotiriou, T. Sannomiya, A. Teleki, F. Krumeich, J. Vörös, S. E. Pratsinis, *Adv. Funct. Mater.* **2010**, *20*, 4250; b) X. Yuan, M. I. Setyawati, D. T. Leong, J. Xie, *Nano Res.* **2014**, *7*, 301; c) M. I. Setyawati, R. V. Kutty, C. Y. Tay, X. Yuan, J. Xie, D. T. Leong, *ACS Appl. Mater. Interfaces* **2014**, *6*, 21822; d) H. Pei, X. Zuo, D. Zhu, Q. Huang, C. Fan, *Acc. Chem. Res.* **2014**, *47*, 550; e) J. Li, C. Fan, H. Pei, J. Shi, Q. Huang, *Adv. Mater.* **2013**, *25*, 4386; f) X. Ouyang, J. Li, H. Liu, B. Zhao, J. Yan, Y. Ma, S. Xiao, S. Song, Q. Huang, J. Chao, C. Fan, *Small* **2013**, *9*, 3082.
[4] United States Environmental Protection Agency, Recreational Water Quality Criteria, http://water.epa.gov/scitech/swguidance/standards/criteria/health/recreation/upload/RWQC2012.pdf (accessed: Mar 2015).
[5] World Health Organization, *Guidelines for Drinking-Water Quality*, 4th ed., http://whqlibdoc.who.int/publications/2011/9789241548151_eng.pdf (accessed: Mar 2015).
[6] a) L. Su, W. Jia, C. Hou, Y. Lei, *Biosens. Bioelectron.* **2011**, *26*, 1788; b) A. T. Sage, J. D. Besant, B. Lam, E. H. Sargent, S. O. Kelley, *Acc. Chem. Res.* **2014**, *47*, 2417; c) R. de la Rica, C. Pejoux, H. Matsui, *Adv. Funct. Mater.* **2011**, *21*, 1018.
[7] K. Abu-Rabeah, A. Ashkenazi, D. Atias, L. Amir, R. S. Marks, *Biosens. Bioelectron.* **2009**, *24*, 3461.
[8] S. Noh, Y. Choe, V. Tamilavan, M. H. Hyun, H. Y. Kang, H. Yang, *Sens. Actuators B* **2015**, *209*, 951.
[9] H. Pei, X. Zuo, D. Pan, J. Shi, Q. Huang, C. Fan, *NPG Asia Mater.* **2013**, *5*, e51.
[10] H. Pei, N. Lu, Y. Wen, S. Song, Y. Liu, H. Yan, C. Fan, *Adv. Mater.* **2010**, *22*, 4754.
[11] L. Yuan, M. Giovanni, J. Xie, C. Fan, D. T. Leong, *NPG Asia Mater.* **2014**, *6*, e112.
[12] A. Chen, B. Shah, *Anal. Methods* **2013**, *5*, 2158.
[13] M. Barreiros dos Santos, J. P. Agusil, B. Prieto-Simón, C. Sporer, V. Teixeira, J. Samitier, *Biosens. Bioelectron.* **2013**, *45*, 174.
[14] X. Guo, A. Kulkarni, A. Doepke, H. B. Halsall, S. Iyer, W. R. Heineman, *Anal. Chem.* **2012**, *84*, 241.
[15] Y. Li, R. Afrasiabi, F. Fathi, N. Wang, C. Xiang, R. Love, Z. She, H.-B. Kraatz, *Biosens. Bioelectron.* **2014**, *58*, 193.
[16] a) Y. Guo, Y. Wang, S. Liu, J. Yu, H. Wang, M. Cui, J. Huang, *Analyst* **2015**, *140*, 551; b) D. Dechtrirat, N. Gajovic-Eichelmann, F. Wojcik, L. Hartmann, F. F. Bier, F. W. Scheller, *Biosens. Bioelectron.* **2014**, *58*, 1.
[17] I.-H. Cho, P. Bhandari, P. Patel, J. Irudayaraj, *Biosens. Bioelectron.* **2015**, *64*, 171.
[18] D. Mendes Silva, L. Domingues, *Ecotoxicol. Environ. Saf.* **2015**, *113*, 400.
[19] A. Wu, P. Ou, L. Zeng, *NANO* **2010**, *05*, 245.